Доклади на Българската академия на науките
Comptes rendus de l'Académie bulgare des Sciences
Tome 77, No 2, 2024

ENGINEERING SCIENCES
Mechanics

EXPLORING LOW-SPEED MARINE DIESEL ENGINE PARAMETERS THROUGH ADVANCED 3D VISUALIZATION WITH DELAUNAY TRIANGULATION

Dimitrichka Nikolaeva[1], Evgeni Nikolaev[1], Radostina Yankova[2], Deyan Veselinov[2]✉

Received on November 10, 2023
Presented by Ch. Roumenin, Member of BAS, on December 19, 2023

Abstract

The article presents an algorithm for creating software leading to the optimization of the combustion process of marine engines. Parameters determining the Existing Ships Energy Efficiency Index (EEXI) related to ship type, capacity, and propulsion principle are considered. Test data on the characteristics of a two-stroke main engine, model HYUNDAI 6S60MC-C for six types of loads were used as the basis. To present the working field of the engine, the necessary calculations have been carried out and dependencies have been derived for the power and the specific fuel consumption as a function of the revolutions. The implementation includes the development of a small software program using Delaunay's triangulation algorithm to create 3D graphics, as well as Python libraries and methods.

Key words: Delaunay triangulation, 3D visualization, EEXI, CII, marine diesel engine, effective power, specific fuel consumption

1. Introduction. The global trade supply chain relies heavily on the international shipping sector, with approximately 80% by volume, and 70% by value of goods being transported by sea vessels [1]. While shipping is considered the most efficient and cost-effective method of international transportation for most goods it is facing growing concerns due to its substantial fuel consumption and the resulting surge in air pollutants including nitrogen oxides (NOx), sulphur

https://doi.org/10.7546/CRABS.2024.02.11

oxides (SOx), harmful particulate matter (PM), and greenhouse gases, primarily carbon dioxide (CO_2). According to reports published by the International Maritime Organization (IMO), international shipping contributes significantly to global emissions, accounting for approximately 14–31% of nitrogen oxide (NOx) emissions, 4–10% of sulphur oxide (SOx) emissions, and 2–3% of carbon dioxide (CO_2) emissions worldwide [2].

Since 2018, the IMO has implemented a strategy aimed at mitigating greenhouse gas emissions originating from ships [3]. In alignment with this strategy, significant amendments are underway within the International Convention for the Prevention of Pollution from Ships (MARPOL). Starting from November 2022, Chapter 4 of Annex VI is undergoing revisions that compel the rapid enhancement of ships' energy efficiency. Furthermore, effective January 1, 2023, the calculation of the Energy Efficiency Existing Index (EEXI) has been mandated, necessitating the collection of data to report an annual operational indicator known as the Carbon Intensity Indicator (CII). Stringent regulations have been introduced, encompassing enhanced inspection protocols, certification requirements, and more robust control mechanisms for various vessel categories. These measures reflect a significant step towards reducing emissions from maritime transport and fostering a decline in the carbon intensity associated with international shipping. To achieve this goal, a substantial reduction of 40% in the Energy Efficiency Existing Index (EEXI) is expected by the year 2030 [4].

Several measures have been implemented to advance this cause, including the adoption of energy-efficient technologies and recycling systems [5], streamlining fuel processes for optimization [6], implementation of hybrid propulsion systems [7], onboard carbon dioxide (CO_2) capture initiatives [8], and the utilization of diverse methods for optimizing the main engine's workload [9]. In the case of vessels currently in operation, reducing carbon dioxide and nitrogen oxide (NOx) emissions often involves the optimization of combustion processes.

Some of the world's largest and most essential maritime vessels, such as container ships and bulk carriers are powered by low-speed diesel engines. These engines are renowned for their robustness and fuel efficiency, making them vital for long-haul and heavy-duty applications. Visualizing the parameters of a low-speed diesel engine is pivotal in the maritime industry. This graphical representation offers a clear insight into engine performance, assisting operators in selecting the most advantageous operating configurations. By visually assessing crucial parameters supplemented when the external sailing conditions, such as wave, wind, and draft change ship operators and engineers can make informed decisions to optimize the engine's performance [10]. This process aids in reducing environmentally harmful emissions, enhancing fuel efficiency, and ultimately promoting the sustainability of maritime operations [11, 12].

This article presents a software program using Delaunay's triangulation algorithm, which calculates the basic parameters of a main engine and presents a

detailed visualization of the engine's operating field, facilitating the selection of an optimal operating point.

2. Principles and tasks formulation. To create a 3D graph illustrating the operational range of a low-speed diesel engine, three key design parameters are considered: specific fuel consumption, effective power output, and engine speed (revolutions per minute). This approach simplifies the process of identifying the optimal operating mode for the engine, making it more accessible and user-friendly for engineers and operators [13].

Additionally, the execution of several essential tasks is necessary:

1. Initial measurements and calculations:

   Building upon initial measurements of the three key characteristics, a series of calculations are executed, dependencies are meticulously established, and graphical representations are crafted. The basic steps involved in the process include:

   - Calculate the effective power ($P_{e\ calc.}$).
   - Determine the specific fuel consumption (be) and its variation as a percentage of the nominal effective power at 100% load (P_e).
   - Create graphical representations and establish dependencies using two reference points.
   - Identify key coefficients, including α, β, μ, μ', σ, σ'.
   - Plot the function be $= f(P_e\ \%)$, generate an approximating curve, and establish correlations.
   - Calculate specific fuel consumption (be) and effective power (P_e) for various load conditions to acquire additional data points.

2. Development of an algorithm to facilitate the creation of a specialized software solution for 3D visualization.

3. Utilization of the algorithm to develop a user-friendly software application tailored for 3D visualization, providing an efficient and practical tool for engine performance analysis.

These comprehensive tasks and software capabilities enhance the precision and efficiency of evaluating low-speed diesel engine operation, offering valuable insights for optimal performance assessment.

3. Experimental setting and results. ***3.1. Initial measurements and calculations.*** Following measurements conducted at a rotation frequency close to the engine's operational speed, the correlation between power and revolutions is established. For performance testing of the two-stroke low-speed diesel engine,

Table 1

Test data of two-stroke low-speed diesel engine HYUNDAI model 6S60MC-C; D – Description, C/M – Calculated/Measured, L – Load (% of P_e), MIP – Mean Indicator Pressure (P_i, [kW]), R – Revolutions per minute (n, [rpm]), EF – Effective power (P_e, [BHP]), HE – Consumption per hour (B_h, [kg/h]), EFC – Effective Power Calculated ($P_{e\ calc.}$), [kW]), SFC – Specific fuel consumption (be, [kg/kWh]), REP – Rated effective power (P_e, % of REP at 100% and load = 11 326.4706 [kW])

D	Row	C/M	Column					
			1	2	3	4	5	6
L	1		25	50	75	90	100	110
MIP	2		8.16	12.37	15.91	17.81	19.06	20.23
R	3	M	61.10	77.00	88.10	93.70	97.00	100.10
EF	4		3849.00	7700.00	11550.00	13868.00	15404.00	16937.00
HE	5		517.1430	1017.3910	1488.5710	1802.8570	2021.6740	2261.2310
EFC	6		2830.1471	5661.7647	8492.6471	10197.0588	11326.4706	12453.6765
SFC	7	C	0.182632	0.179648	0.175232	0.176858	0.178491	0.181492
REF	8		2831.617647	5663.235294	8494.852941	10193.82353	11326.47059	12459.11765

specifically the HYUNDAI 6S60MC-C model, data was collected for six different load conditions, as outlined in Table 1.

Subsequently, comprehensive calculations are performed to create a visual representation of the engine's operational range. This graphical presentation effectively conveys the interplay between engine revolutions, power output, and specific fuel consumption. The sequence of calculations is in the following order:

First, convert effective power from horsepower to kilowatts using:

$$P_{e\ calc.}[\mathrm{kW}] = \frac{P_e[\mathrm{BHP}]}{1.36}. \tag{1}$$

The calculated results are shown in row 6 of Table 1.

Next, the calculation of the specific fuel consumption is performed using:

$$\mathrm{be}_i \left[\frac{\mathrm{kg}}{\mathrm{kWh}}\right] = \frac{B_{h_i}}{P_{e_i}} \left[\frac{\mathrm{kg}}{\mathrm{kWh}}\right], \tag{2}$$

where the specific fuel consumption be is calculated as the ratio between the hourly consumption B_{h_i} and the effective power P_{e_i} at different loads i. Calculated results for $i = 25\%$, 50%, 75%, 90%, 100%, and 110% are available in Table 1, row 7.

Calculating the coefficients α, β, μ, σ, μ', σ', under specific conditions of the ship engine complex helps to solve the task of choosing the optimal operating mode. Using them it is possible to determine graphical dependencies for power (P_e), and velocity of the ship (V_s) at specific revolutions (n).

The coefficients β and μ, which characterize the ship screw, are determined to calculate the effective power using the following equation

$$P_e = \mu * n^{\beta}, \tag{3}$$

where P_e is the effective power of the engine, [kW]; μ is the coefficient characterizing the ship screw; β is the coefficient characterizing the ship screw, within the range $2.6 < \beta < 3.3$; and n is the number of revolutions per minute [rpm].

Based on the assumption that if two mode points lie on the same screw characteristic, it follows that $\beta_1 = \beta_2$ and $\mu_1 = \mu_2$. The coefficients β and μ are calculated for each point of the screw characteristic using:

$$\beta = \frac{\lg(P_{e,1}/P_{e,2})}{\lg(n_1/n_2)}, \quad \mu = P_e/n^{\beta}. \tag{4}$$

The function be $= f(P_e\ \%)$ is graphed and an approximating curve and correlation are generated (Fig. 1).

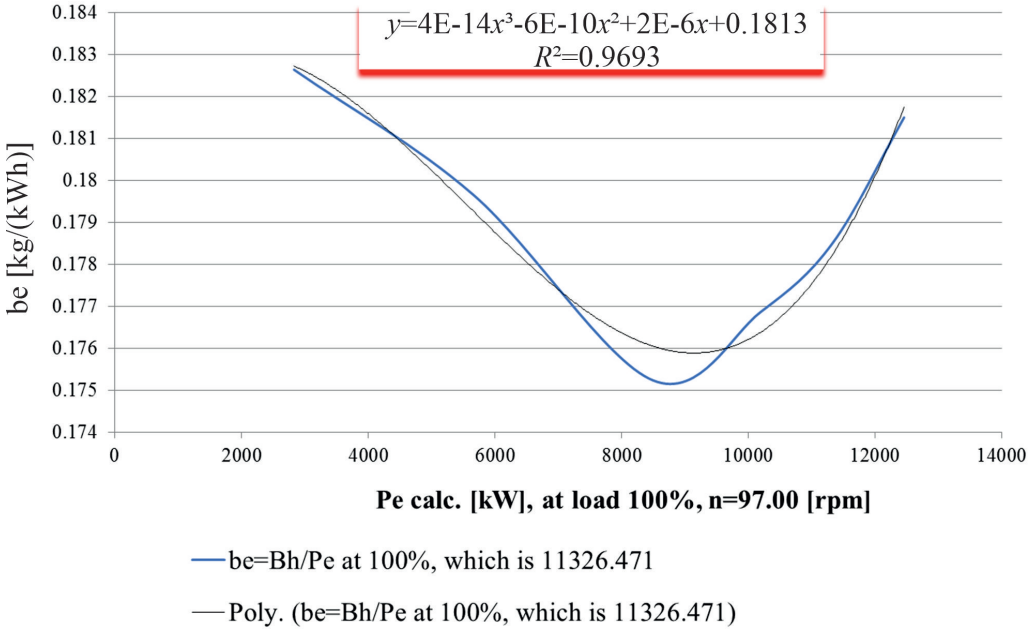


Fig. 1. Generated approximating curve and correlation for specific load flow

An equation of the form is derived:

$$y = 4\mathrm{E} - 14 * x^3 - 6\mathrm{E} - 10 * x^2 + 2\mathrm{E} - 06 * x + 0.183 \tag{5}$$

and correlation:

$$R^2 = 0.969. \tag{6}$$

After substituting into the equation be $= f(P_e\ \%)$ the resulting formula is:

$$\mathrm{be} = 4 * \mathrm{E} - 14 * P_e^3 - 6 * \mathrm{E} - 10 * P_e^2 + 2 * \mathrm{E} - 06 * P_e + 0.183. \tag{7}$$

Table 2

Calculated and summarized results

%	n	P_e	be	%	n	P_e	be
25	61.1	2789.868	0.184778	90	93.7	2836.865	0.184758
25	61.1	5579.737	0.182428	90	93.7	5673.730	0.182339
25	61.1	8369.605	0.181161	90	93.7	8510.595	0.181220
25	61.1	10043.530	0.183088	90	93.7	10212.710	0.183453
25	61.1	11159.470	0.186188	90	93.7	11347.460	0.186882
25	61.1	12275.420	0.191129	90	93.7	12482.210	0.192273
50	77.0	2814.478	0.184768	100	97.0	2835.964	0.184759
50	77.0	5628.957	0.182381	100	97.0	5671.928	0.182340
50	77.0	8443.435	0.181190	100	97.0	8507.892	0.181219
50	77.0	10132.120	0.183275	100	97.0	10209.470	0.183446
50	77.0	11257.910	0.186545	100	97.0	11343.860	0.186868
50	77.0	12383.710	0.191718	100	97.0	12478.240	0.192250
75	88.1	2823.563	0.184764	110	100.1	2836.420	0.184758
75	88.1	5647.126	0.182364	110	100.1	5672.840	0.182339
75	88.1	8470.689	0.181202	110	100.1	8509.260	0.181219
75	88.1	10164.830	0.183346	110	100.1	10211.110	0.183449
75	88.1	11294.250	0.18668	110	100.1	11345.680	0.186875
75	88.1	12423.680	0.191941	110	100.1	12480.250	0.192262

Table 2 shows the summarized results for effective power and specific fuel consumption as a function of rpm.

3.2. Development of an algorithm to facilitate the creation of a specialized software solution for 3D visualization.

3.2.1. Delaunay triangulation and application. Delaunay triangulation is a geometric algorithm widely employed in computational geometry to efficiently partition a set of points into non-overlapping triangles. Its application extends to 3D visualization, where it becomes a powerful tool for representing and analyzing complex spatial relationships. In the context of 3D visualization, Delaunay triangulation aids in creating a well-defined network of tetrahedra, connecting points in three-dimensional space. This process not only enhances the visualization of intricate surfaces but also facilitates the interpolation of data across the 3D domain. The resulting triangulation forms the basis for constructing surfaces and volumes, providing a structured framework that proves invaluable in various fields, including computer graphics, geographical information systems, and, notably, the representation of parameters in engineering systems such as marine diesel engines [14, 15].

3.2.2. Creating an algorithm for 3D visualization. The algorithm for 3D visualization encompasses several key steps. Initially, input data is loaded from

an Excel file, facilitating organized data management. Subsequently, the algorithm organizes the visualization of this data in a tabular format for enhanced accessibility. The process then involves the establishment of a network of coordinates, incorporating both $f(P_e, n)$ coordinates and relative coordinates within a 2D plane. Leveraging the triangulation method grounded in the Delaunay algorithm, the algorithm systematically generates a comprehensive spatial representation. This method proves particularly instrumental in constructing a 3D visualization that vividly illustrates the energy performance of a low-speed marine diesel engine. By seamlessly integrating data coordination and triangulation, the algorithm enhances the interpretability and utility of the visualization, fostering a more insightful understanding of the engine's operational dynamics.

3.2.3. Implementation of libraries for 3D rendering. The development of the software for 3D visualization of low-speed marine diesel engine parameters, based on Delaunay triangulation, employed the versatile Python programming language. Several key libraries played a crucial role in this implementation. `Numpy`, a powerful numerical computation library, facilitated the handling of large multidimensional arrays and provided essential mathematical functions [16]. `Matplotlib`, an extensive plotting library, served as the backbone for 2D visualizations, offering static, animated, and interactive graphics capabilities [17]. The `mpl_toolkits` library was instrumental in generating 3D graphics using the `mplot3d` module. `Tkinter`, as the standard Python interface to the `Tcl/Tk` GUI toolkit, ensured seamless interaction with graphical elements [18]. `Pandas`, a data manipulation library, complemented `Matplotlib` by providing a memory-efficient 2D data table object known as a `Dataframe`. The `openpyxl` library, designed for reading and writing Excel files, facilitated efficient data analysis and extraction [19].

In terms of methods, the software leveraged various functionalities from `Matplotlib` and related modules. The `matplotlib.tri` module facilitated the handling of unstructured triangular networks, while `fig.add_subplot()` was utilized to add axes to the figure [17]. The `ax.scatter()` method allowed for the plotting of scatterplots, providing a visual representation of the relationships between variables [20]. The `mtri.Triangulation()` method, rooted in trigonometry and elementary geometry, contributed to determining distances using the geometry of triangles. Additionally, `ax.triplot()` and `ax.plot_trisurf()` were employed to visualize unstructured triangular meshes in 2D and 3D, respectively. The `ax.view_init()` method enabled programmatic rotation of the axes, enhancing the interactive visualization experience. Furthermore, the software utilized `matplotlib.pyplot.get_cmap` to define a `colormap` instance, and `fig.colorbar()` added a color bar for improved data interpretation. Finally, `ax.set_title`, `ax.set_xlabel`, and other similar methods were employed to enhance the visual clarity of the generated plots.

In addition to libraries and methods, the use of arrays, a new data type in Python, significantly enhanced the efficiency of the software. Utilizing NumPy's

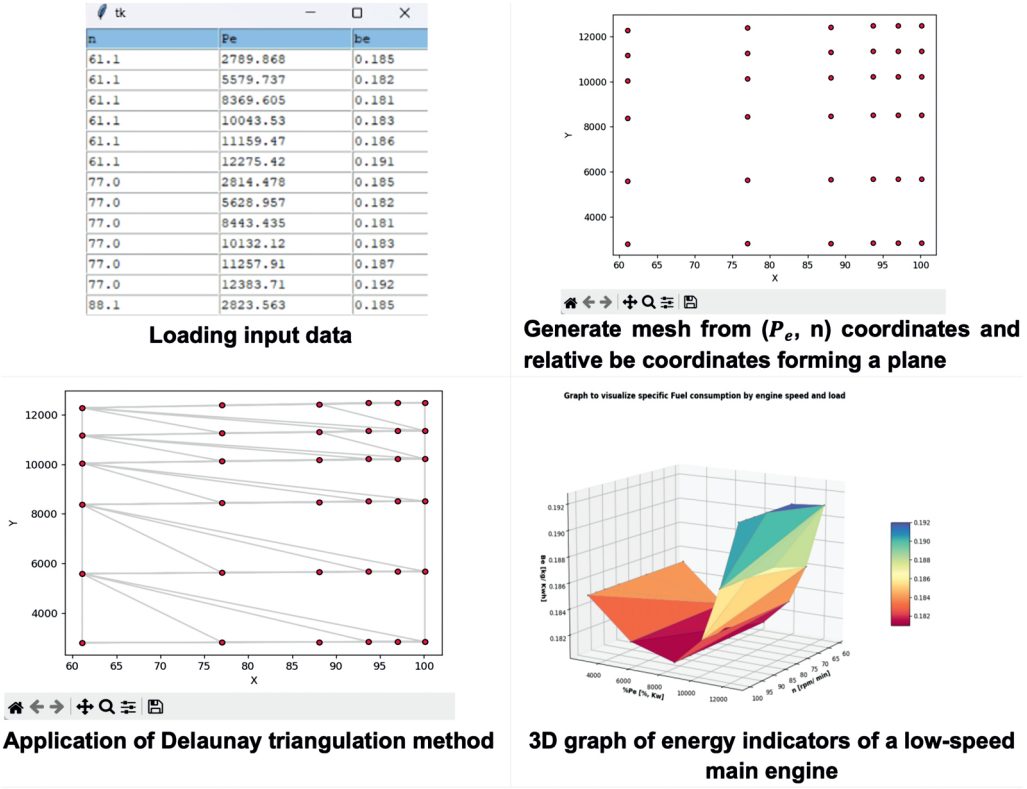


Fig. 2. Screenshots of 3D visualization of low-speed diesel engine parameters based on Delaunay triangulation

`array()` function, the software created arrays and ordered collections of elements of the same type, a feature particularly beneficial for handling and analyzing large datasets within the context of 3D visualization.

Figure 2 summarizes four primary screen interfaces of the deployed 3D visualization software.

4. Conclusion. The article addresses a key concern in the shipping industry in recent years, specifically focusing on the imperative reduction of carbon emissions into the atmosphere. A pivotal stride in this direction involves the development of a 3D visualization utilizing the Delaunay triangulation algorithm. This visualization effectively illustrates the intricate relationships among specific fuel consumption, main engine speed, and power. The study leverages data from tests conducted on six distinct loads using the HYUNDAI 6S60MC-C model. Through rigorous calculations, mode coefficients were determined, and a function, be $= f(P_e\ \%)$, was graphed, resulting in the generation of an approximating curve and correlation. This methodology has culminated in the creation of an algorithm, forming the basis for a compact 3D visualization software based on Delaunay triangulation. Looking ahead, the program has the potential for expansion,

accommodating diverse ship types and variations in main engine characteristics as part of its future development.

REFERENCES

[1] Gray N., S. McDonagh, R. O'Shea, B. Smyth, J. D. Murphy (2021) Decarbonising ships, planes and trucks: An analysis of suitable low-carbon fuels for the maritime, aviation and haulage sectors, Adv. Appl. Energy, **1**, 100008, https://doi.org/10.1016/J.ADAPEN.2021.100008.

[2] Faber J., S. Hanayama, S. Zhang, P. Pereda, B. Comer et al. (2021) Fourth IMO GHG Study 2020, Full Report, London, https://greenvoyage2050.imo.org/wp-content/uploads/2021/07/Fourth-IMO-GHG-Study-2020-Full-report-and-annexes_compressed.pdf.

[3] International Maritime Organization (2018) Initial IMO strategy on reduction of GHG emissions from ships, https://unfccc.int/sites/default/files/resource/250_IMOsubmission_TalanoaDialogue_April2018.pdf.

[4] International Maritime Organization (n.d.) EEXI and CII – ship carbon intensity and rating system, https://www.imo.org/en/MediaCentre/HotTopics/Pages/EEXI-CII-FAQ.aspx (accessed November 8, 2023).

[5] Yuan C., P. Pan, Y. Sun, X. Yan, X. Tang (2021) The evaluating on EEDI and fuel consumption of an inland river 800PCC integrated with solar photovoltaic system, J. Mar. Eng. Technol., **20**, 77–92, https://doi.org/10.1080/20464177.2019.1571671.

[6] Winterthur Gas & Diesel Ltd. (2017) Marine Installation Manual.

[7] Gallucci M. (2018) The struggle to make diesel-guzzling cargo ships greener IEEE Spectrum, https://spectrum.ieee.org/the-struggle-to-make-dieselguzzling-cargo-ships-greener?utm_campaign=climatetechsub#toggle-gdpr (accessed November 6, 2023).

[8] Lee S., S. Yoo, H. Park, J. Ahn, D. Chang (2021) Novel methodology for EEDI calculation considering onboard carbon capture and storage system, Int. J. Greenh. Gas Control., **105**, 103241, https://doi.org/10.1016/J.IJGGC.2020.103241.

[9] Reusser C., M. A. Perez, J. P. Osses (2018) Ship's PTO/PTI Torque Field Oriented Control scheme, with optimization strategy, for EEDI index improvement. In: 2018 IEEE Int. Conf. on Electrical Systems for Aircraft, Railway, Ship Propulsion and Road Vehicles and International Transportation Electrification Conference, ESARS-ITEC, https://doi.org/10.1109/ESARS-ITEC.2018.8607745.

[10] Shi W., H. T. Grimmelius, D. Stapersma (2010) Analysis of ship propulsion system behaviour and the impact on fuel consumption, Int. Shipbuild. Prog., **57**, 35–64, https://doi.org/10.3233/ISP-2010-0062.

[11] Finger G., A. U. Schubert, T. Riebe, S. Fischer, M. Gluch et al. (2020) Consumption and Emission Minimised Ship Manoeuvring. In: Global Oceans 2020: Singapore – US Gulf Coast, Biloxi, MS, USA, 6 pp, https://doi.org/10.1109/IEEECONF38699.2020.9389278.

[12] Alif H. H., W. P. Sari, B. M. Sopha, A. Aprilana, Y. P. Mulyani et al. (2022) Specific fuel consumption prediction model for diesel engines: a preliminary study. In: IEEE Int. Conf. on Industrial Engineering and Engineering Management 2022, 497–501, https://doi.org/10.1109/IEEM55944.2022.9989866.
[13] Wilson D. E. (1986) The design of a low specific fuel consumption turbocompound engine, SAE Technical Papers, https://doi.org/10.4271/860072.
[14] Geometry in Action: Delaunay Triangulation, https://ics.uci.edu/~eppstein/gina/delaunay.html (accessed November 7, 2023).
[15] Xenitidis K., K. Ioannou, G. Tsantopoulos (2023) An innovative methodology for the determination of wind farms installation location characteristics using GIS and Delaunay Triangulation, Energy Sustain. Dev., **75**, 25–39, https://doi.org/10.1016/J.ESD.2023.05.006.
[16] NumPy Documentation (n.d.) NumPy v1.26 Manual, https://numpy.org/doc/stable/ (accessed November 10, 2023).
[17] Remi M. (2021) ActiveState (n.d.) What is Matplotlib in Python? How to use it for plotting?, https://www.activestate.com/resources/quick-reads/what-is-matplotlib-in-python-how-to-use-it-for-plotting/ (accessed November 10, 2023).
[18] Python 3.12.0 Documentation (n.d.) Graphical User Interfaces with Tk, https://docs.python.org/3/library/tk.html (accessed February 12, 2024).
[19] Gazoni E., C. Clark (2023) openpyxl 3.1.2 Documentation, openpyxl – A Python library to read/write Excel 2010 xlsx/xlsm files, https://openpyxl.readthedocs.io/en/stable/ (accessed November 10, 2023).
[20] Clinical Excellence Commission (n.d.) Scatter Plot, https://www.cec.health.nsw.gov.au/CEC-Academy/quality-improvement-tools/scatter-plot (accessed November 10, 2023).

[1] *Technical University of Varna, 1 Studentska St, 9010 Varna, Bulgaria*
e-mails: d.nikolaeva@tu-varna.bg, evgeny1@abv.bg

[2] *Institute of Metal Science, Equipment and Technologies with Hydro- and Aerodynamics Centre "Acad. A. Balevski", Bulgarian Academy of Sciences,*
67 Shipchenski Prohod Blvd, 1574 Sofia, Bulgaria
e-mails: radyankova@ims.bas.bg, dveselinov@ims.bas.bg